

## Seismic AVO Modeling Using In situ Samples for Reservoir Study

Esmailpour, S.<sup>1\*</sup>, Riahi, M. A.<sup>2</sup>, Emamzadeh, A.<sup>3</sup> and Sokooti, R.<sup>4</sup>

<sup>1</sup>M. Sc. Student of Geophysics, ISP- School, Paris, France

<sup>2</sup>Associate Professor, Earth Physics Department, Institute of Geophysics, University of Tehran, Iran

<sup>3</sup>Associate professor, petroleum engineering department, Petroleum university of technology, Tehran, Iran

<sup>4</sup>M. Sc. of Geophysics, Oil Exploration Director, National Iranian Oil Company, Tehran, Iran

(Received: 22 Nov 2006, Accepted: 12 May 2009)

### Abstract

Distinguishable amplitude phenomena on surface seismic data often resulted from contrasts in the elastic parameters of subsurface layers. Various techniques have been involved to analyze and highlight such phenomena for their potential use as "Direct Hydrocarbon Indicator (DHI)". More recently, other techniques have been developed based on the variation of reflection coefficient with angle of incidence, conventionally called Amplitude-Versus-Offset (AVO).

During the last twenty years the significance of AVO analysis for studying seismic reflection in oil exploration has been considered more importantly.

In this work, first, a seismic line from a gas field and also a well are selected to indicate the results of the application of AVO analysis for detection of hydrocarbon reservoir in this field.

In this project, using well logs and information obtained by core analysis, a synthetic seismogram has been built applying Zoeppritz equation. And Using Hampson-Russell software, AVO attributes have been extracted from synthetic seismogram. Then anomalies of these attributes have been investigated and compared with the anomalies from AVO attributes which were extracted from real seismic data to characterize the reservoir.

It has been seen that the extracted attributes of the synthetic seismogram confirm the anomalies from real seismic data.

Finally according to the obtained result, observed anomalies can be interpreted as a Gas Cap for this reservoir.

This study is useful to identify reservoir and nonreservoirs and the results of this study are considered as input for detailed reservoir studies. In particular, knowing the reservoir physical and saturating fluid properties is of great importance in making plans for developing the reservoir.

**Key words:** AVO, Attribute, Shear wave velocity, Compressional wave velocity, Offset, Pre-stack, Synthetic seismogram

### مدلسازی لرزه‌ای AVO با استفاده از داده‌های مغزه برای مطالعه مخزن

سجاد اسماعیل‌پور<sup>۱\*</sup>، محمدعلی ریاحی<sup>۲</sup>، ابوالقاسم امامزاده<sup>۳</sup> و رضا سکوتی<sup>۴</sup>

<sup>۱</sup> دانشجوی کارشناسی ارشد مهندسی اکتشاف نفت، انستیتو نفت، فرانسه، پاریس

<sup>۲</sup> دانشیار، گروه فیزیک زمین، مؤسسه ژئوفیزیک، دانشگاه تهران، ایران

<sup>۳</sup> دانشیار، گروه مهندسی نفت، دانشگاه تحصیلات تکمیلی صنعت نفت، تهران، ایران

<sup>۴</sup> کارشناس ارشد ژئوفیزیک، مدیریت اکتشاف نفت، شرکت ملی نفت ایران، تهران، ایران

(دریافت: ۸۵/۹/۱، پذیرش نهایی: ۸۸/۲/۲۲)

## چکیده

امروزه به کارگیری آنالیز تغییرات دامنه لرزه‌ای با دورافت (AVO) در تفسیر کیفی و به‌ویژه کمی داده‌های لرزه‌ای از مراحل اولیه اکتشافات مخازن هیدروکربوری گرفته تا تولید آنها، جایگاه ویژه‌ای در صنایع بالادستی نفت را به خود اختصاص داده است. استخراج خواص مخزنی شامل: تخلخل، محتوای سیال، فشار، جداسازی مرز سیالات هیدروکربوری در مخزن، تعیین رخساره‌های سنگی (به‌ویژه شیلی) و تعیین جهت و چگالی شکستگی‌های مخزنی و همچنین تعیین خواص کشسانی سنگ مخزن شامل مدول یانگ، مدول بالک، ضریب پواسون و مانند آن از جمله کاربردهای استفاده از آنالیز تغییرات دامنه لرزه‌ای با دورافت است.

آنالیز تغییرات دامنه لرزه‌ای با دورافت با به کارگیری نشانگرهای لرزه‌ای ویژه، در شبیه‌سازی هرچه دقیق‌تر مخزن، روش‌های تحقیقاتی متداول لرزه‌ای را تحت‌الشعاع قرار داده است. با استفاده از این آنالیز، شناسایی مستقیم هیدروکربورهای گازی و تعیین سطح جدایش سیالات مخزنی امکان‌پذیر است و بدین ترتیب مخاطره اکتشافات نفت و گاز به میزان قابل توجهی کاهش می‌یابد. همچنین نتایج حاصل از آنالیز AVO می‌تواند به‌منظور اجرای تحقیقات پیشگیری لرزه‌ای (چهاربُعدی) و اجرای هر چه بهینه‌تر روش‌های ازدیاد برداشت در مراحل بعدی توسعه‌ای و تولیدی مورد استفاده قرار گیرد.

در این پروژه در مدل‌سازی مستقیم با استفاده از روابط زوپریتس (۱۹۱۹)، شوی (۱۹۸۵) و دیگران و به کارگیری نمودارهای صوتی (تراکمی و برشی) و چگالی، لرزه‌نگاشت مصنوعی با دورافت برای چاه‌های موجود ساخته می‌شود. از آنجاکه اندازه‌گیری نمودار صوتی از امواج برشی بسیار پرهزینه است، در مواردی که این نمودار در اختیار نباشد، با به کارگیری روابط فیزیک‌سنگی نظری و تجربی که پیچیدگی‌های سنگ مخزن در آنها لحاظ شده باشد، مانند معادله بیوت-گسمن و معادله کاستر-توکسوز، برآورد می‌شود و برای ساخت لرزه‌نگاشت مصنوعی با دورافت، مورد استفاده قرار می‌گیرد. در تحقیق حاضر، این داده‌ها با کمک نتایج حاصل از آنالیز مغزه در آزمایشگاه محاسبه شده است. در ادامه با کمک نگارهای چاهی با روش معادله زوپریتس مدل لرزه‌ای قبل از استک ساخته می‌شود. سپس به استخراج نشانگرها روی مدل مصنوعی می‌پردازیم. در پایان مدل لرزه‌ای مصنوعی و بی‌هنجاری‌های شناخته شده را با بی‌هنجاری‌های AVO آشکار شده در نشانگرهای استخراج شده از داده‌های لرزه‌ای واقعی، مقایسه و بررسی می‌کنیم و از آنها در شناسایی مستقیم هیدروکربن در مخزن بهره می‌گیریم. همچنین پس از این تحقیق، برای سازند مورد بررسی و در مناطق مشابه، لاگ سرعت موج برشی با استفاده از لاگ سرعت موج فشارشی قابل برآورد خواهد بود.

واژه‌های کلیدی: تغییرات دامنه لرزه‌ای با دورافت (AVO)، نشانگرهای لرزه‌ای، سرعت امواج لرزه‌ای برشی و طولی، دورافت، پیش

از برانبارش، لرزه نگاشت مصنوعی

## 1 INTRODUCTION

Exploration geophysics is, to a large extent, a science of anomalies. It is probably safe to assume that most hydrocarbons found in the past fifty years have been associated with some kind of geophysical anomaly. (Foster, et al., 1993)

Ostrander (1982) demonstrated that gas sand reflection coefficients vary in an anomalous fashion with increasing offset and showed how to utilize this anomalous behavior as a direct hydrocarbon indicator on real data. This work popularized the methodology which has come to be known as amplitude variation with offset analysis (AVO). (Castagna et al., 1985).

Theory and laboratory measurements indicate that gas sands tend to exhibit abnormally low Poisson's ratios. (Bortfeld, 1961)

Embedding low velocity gas sand into

sediments having 'normal' Poisson's ratios should result in an increase in reflected P-wave energy with an angle of incidence. This phenomenon has been observed on conventional seismic data recorded over known gas sands. (Castagna et al., 1985).

Explorationists are successfully using AVO anomalies to find hydrocarbons throughout the world. The explorationist does not require answers that are correct in absolute terms. The presence of a deviation from some background trend may be sufficient; the magnitude of the deviation in absolute units may not even be required. (Castagna et al., 1993)

In AVO forward modeling, a pre-stack synthetic section is needed. The pre-stack synthetic section is a convolution of Vs, Vp and  $\rho$  with the source wavelet. Unfortunately the Vs data for this process is not available.

For obtaining Vs; information from eight cores that have been taken from this gas reservoir, have been used. This information includes Vp and Vs. With regression of the obtained data, Vp and Vs, an equation has been derived which represents the relation between Vp and Vs in this gas sand.

Determining this equation, we can finally obtain the Vs from Vp log and therefore construct the pre-stack seismogram.

## 2 BACKGROUND

### 2-1 Zoeppritz Equations

The Zoeppritz equations are the basis of AVO analysis. They allow us to derive the exact plane wave amplitudes of a reflected P-wave as a function of angle.

$$R(\theta) = \frac{1}{2} \left( \frac{\Delta\alpha}{\alpha} + \frac{\Delta\rho}{\rho} \right) - 2 \frac{\beta^2}{\alpha^2} \left( 2 \frac{\Delta\beta}{\beta} + \frac{\Delta\rho}{\rho} \right) \sin^2 \theta + \frac{1}{2} \frac{\Delta\alpha}{\alpha} \tan^2 \theta \quad (1)$$

There are many approximations for the Zoeppritz equation. Notice that all of these approximations can be expressed by the following simple equation (Castagna et al., 1985):

$$R(\theta) = R_p + G \sin^2 \theta \quad (2)$$

This equation is linear if we plot R as a function of  $\sin^2 \theta$ . We could then perform a linear regression analysis on the seismic amplitudes to come up with estimates of both intercept  $R_p$ , and gradient G. But first we must transform our data from constant offset form to constant angle form. Then by measured  $R_p$  and G as two main attributes we can do all AVO processing on real or synthetic data (Gelfand and Larner, 1986).

### 2-2 Synthetic Seismogram

A synthetic seismogram consists of a series of traces that represent the effect of recording seismic data over the one-dimensional earth model. Each trace is calculated independently, assuming that both the source and receiver are at the surface of the earth (Castagna and Bakus, 1997)

The main method of calibrating a seismic record and identifying lithology for stratigraphic interpretation is by creating a

synthetic seismogram from borehole measurements. The logs used for this are the sonic (acoustic velocity) and the density logs. Some other logs are useful for establishing specific lithologies with depth.

## 3 PETROPHYSICAL BASIS IN AVO

Gassmann's (1985) equations provide the fundamental basis for direct hydrocarbon indication. These equations predict a large drop in P-wave velocity and a small increase in S-wave velocity when even a small amount of gas is introduced into the pore space of a compressible brine-saturated sand. This drop (along with the corresponding density change) changes the P-wave reflection coefficient (resulting in "bright" or "dim" spots) and causes a drop in Vp/Vs (which causes AVO anomalies) (Bortfeld, 1961).

Vp-Vs relations are key to the determination of lithology from seismic or sonic log data as well as for direct seismic identification of pore fluids using, for example, AVO analysis.

In practice, the Vp/Vs ratio allows the calculation of the Poisson's ratio, which is a good indicator of the lithology, especially since:

It can be used to differentiate unconsolidated rocks from consolidated rocks.

It can indicate the presence of hydrocarbons (gas saturated sandstones). Figure 1 shows a plot of Poisson's ratio versus  $\alpha$  (P-wave Velocity) to  $\beta$  (S-wave Velocity) ratio (Castagna et al., 1998).

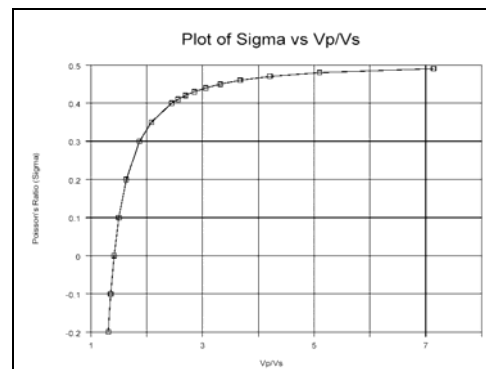


Figure 1. Poisson's ratio as a function of P-wave to S-wave ratio (Castagna et al., 1998).

**3-1 Castagna’s Relationship**

The Biot-Gassmann model for Vs is mathematically complex. Also, the theory falls down when applied to fine grain clastic rocks, such as mudstones. In this case, Castagna et al.(1985) derived a much simpler empirical relationship between P-wave and S-wave velocity, which can be written:

$$\alpha = 1.16 \beta + 1.36 \tag{3}$$

where velocity is in km/s.

There is a wide and sometimes confusing variety of published Vp-Vs relations and Vs prediction techniques, which at first appear to be quite distinct. However, most reduce to the same two simple steps:

- 1) Establish empirical relations among Vp, Vs, and porosity,  $\phi$ , for one reference pore fluid - most often water-saturated or dry.
- 2) Use Gassmann’s (1951) relations to map these empirical relations to other pore-fluid states.

The most reliable and most often used Vp-Vs relations are empirical fits to laboratory or log data, or both.

Figure 2, shows laboratory Vp-Vs data for water-saturated sandstones.

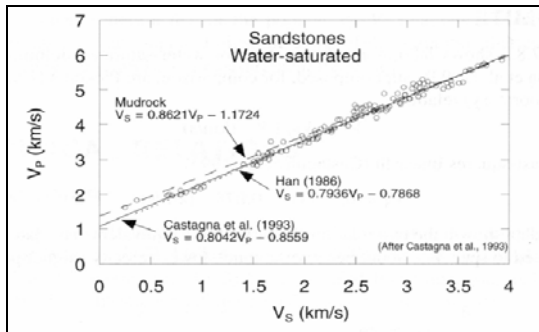


Figure 2. Laboratory Vp-Vs data for water-saturated sandstones (Ross, 2000).

**3-2 A New Empirical Relationship**

At this part of our work, we used 8 cores in depth range of 633m up to 641m which is the interval where we identified it as gas sand in this gas field.

In fact in the laboratory for water saturated cores, the P-wave and S-wave velocities were extracted and the following results were obtained.

Table 1. Laboratory results for 8 cores in the gas sand interval.

Depth(m)	VP(km/s)	VS(km/s)
633.5	2.306	0.834
634.5	2.65	1.192
635.5	2.273	0.835
636.5	3.003	1.4
637.5	2.404	0.88
638.5	2.376	0.9
639.5	2.353	0.92
640.5	2.544	1.003

Figure 3 shows, laboratory ultrasonic Vp-Vs data for water saturated sand stone.

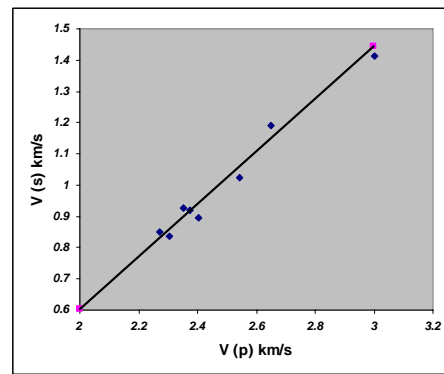


Figure 3. Empirical linear regression from laboratory ultrasonic Vp-Vs data for water saturated sand stone.

This empirical sandstone relation was derived from laboratory core data:

$$Vs = 0.844 Vp - 1.086 \tag{4}$$

where we will use this linear equation in the next section to extract S-wave velocity log from P-wave velocity log, to produce a synthetic seismogram.

**4 CASE STUDY**

AVO (one of the Hampson-Russell software’s modules) is a program used to analyze pre-stack seismic data for the purpose of evaluating and modeling Amplitude Versus Offset anomalies. The input data for this process consists of the following elements:

- One or more well logs.
- A pre-stack seismic volume, either 2D or 3D. This volume has usually been processed to the final CDP gather stage.

The AVO modeling was started, by selecting this program. To start modeling, we must allocate a well which will be used to create the AVO synthetic seismograms and specify which logs will be used to define the model. In our case we have only one p-wave velocity log and one density log available. We also know that offset dependent synthetics can only be created using a P-wave velocity log, a density, and an S-wave velocity log. In our case, there is no S-wave log and in this part we used our derived linear transform equation between  $V_p$  and  $V_s$  from laboratory measurement among 8 core samples and now it is possible to make a shear-wave velocity log, using real P-wave velocity log.

The AVO Modeling window now contains all the logs required to create the offset synthetic. Then a synthetic has been created using these logs. This operation will create an offset-dependent synthetic using ray-tracing to calculate the incidence angles and the Zoeppritz equations to calculate the amplitudes. Only the primary reflection events have been modeled. A synthetic seismogram has been created with 11 offsets ranging from 0 to 600 meters. A Target zone has been set from 600 to 700 meters. This means that the Zoeppritz equations have been used to calculate reflection coefficients for any interface within this depth range (600-700m), but for all interfaces outside this depth range, the zero-offset reflection coefficient has been used to save computation time.

In figure 5, the calculated seismogram has appeared in the AVO Modeling window.

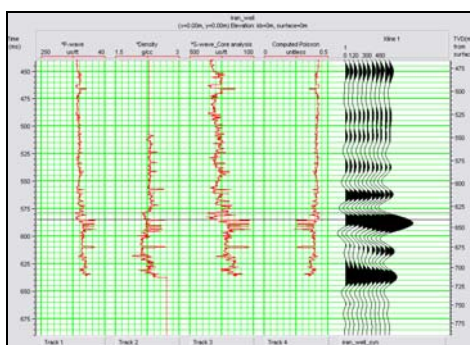


**Figure 5.** Calculated seismogram in the AVO Modeling window.

After the creation of a synthetic seismogram, it has been compared with the real seismic data which ties this well.

There were around 130 CDP gathers on one Xline on which X-well has been located. Each CDP has been named by a number, which has been shown at the top. And X-well is located at CDP 330. In figure 6, a portion of the seismic data has been displayed close to the synthetic seismogram. And CDP330 has been compared with the synthetic seismogram.

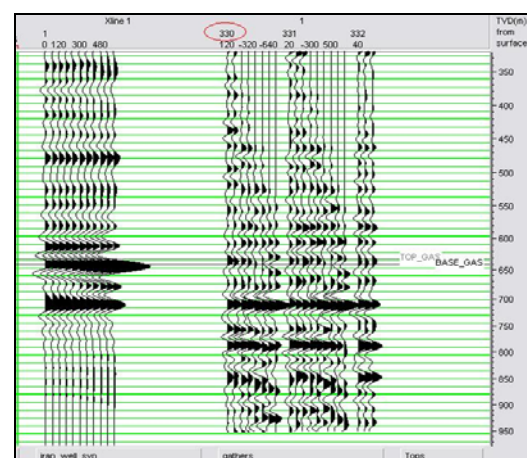


**Figure 6.** CDP 330 and created Synthetic seismogram.

Several ways has been seen in which the synthetic seismogram and seismic data differ. One obvious way is that the times of events on the synthetic seismogram do not correspond to the times of the same events on the seismic. This difference arises because the synthetic seismogram has been created using a default wavelet, which is not necessarily compatible with the wavelet in the seismic data. A new wavelet has been extracted consequently with the Statistical Wavelet Extraction method, which uses the seismic data alone to calculate a zero-phase wavelet whose amplitude spectrum matches that of the seismic.

The last operation which we performed in this section was Log Correlation. This is the process of correcting the depth-time curve which was used to calculate the synthetic seismogram. Figure 7 represents the new synthetic seismogram.

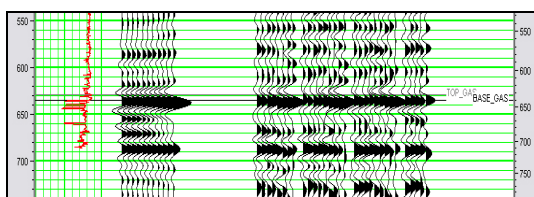


Figure 7. New synthetic seismogram after correlation.

#### 4-1 Performing Fluid Replacement Modeling

Now it was obvious that a major difference between the calculated synthetic seismogram and the real data is that the synthetic seismogram did not show any appreciable AVO behavior, while the real data did. The reason for this was that when we calculated the S-wave log using our derived equation, we effectively modeled the entire log as a wet (brine-filled) log. To calculate the correct S-wave behavior for the gas sand, we need to use Fluid Replacement Modeling (FRM).

To calculate the proper effective S-wave velocity corresponding to the in situ gas case, we specified that the Water Saturation within the target layer is 50%, which effectively means 50% hydrocarbon. Also, we have specified that our derived equation is assumed to be correct for the wet sand case. Within the FRM module, the Biot-Gassmann equations were used to convert the actual P-wave log within the target layer from the 50% water saturation to 100% water saturation. Then, our derived equation was used to calculate the correct shear-wave velocity for the layer at this water saturation. Finally, the Biot-Gassmann equations were used again to correct from the 100% saturation case back to 50%, which is what we desire. Also, we did not specify the porosity within the zone, but allowed the program to calculate it from the other parameters, assuming the measured density in the log density is the true bulk density for the gas layer.

Finally the S-wave velocity and the resulting Poisson's Ratio log were modified effectively within the target zone. Note that the effect of assuming the 50% gas saturation was to lower the Poisson's Ratio within the target zone. Figure 8 represents the new

synthetic seismogram after modification of two above logs.

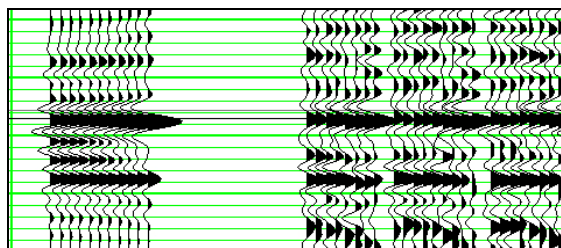


Figure 8. New Synthetic seismogram after FRM.

#### 4-2 AVO Attributes on the generated Gas Synthetic Seismogram

Now it is possible to apply conventional AVO analysis to this synthetic seismogram. In fact, all the AVO processing normally applied to real data can now be tested on the synthetic seismogram data.

The first AVO process was applied, which was the calculation of the intercept and gradient attributes. In particular, note that the program automatically knows the correct velocities from the P-wave velocity log to use for the angle calculations.

We used more inlines of gas synthetic seismogram and also used a wet synthetic seismogram close to the gas synthetic seismogram to improve the visual display and to see differences between gas and wet cases, to find a way for distinguishing different fluids in the reservoir. Two synthetic seismograms (gas and wet models) have been merged into a single volume. Also, we copied each gather an additional 4 times (5 gas synthetic seismograms followed by the 5 wet synthetic seismograms).

When the calculation was finished, the result was displayed in a new window (figure 9). This option has actually calculated two files, one containing the intercept (A) and one containing the gradient (B). Both files are displayed simultaneously in the new window. The Wiggle Data is the intercept (A), while the Data highlighted in color is the product of intercept and gradient ( $A*B$ ). This is usually the best AVO attribute to distinguish Class III AVO anomalies.

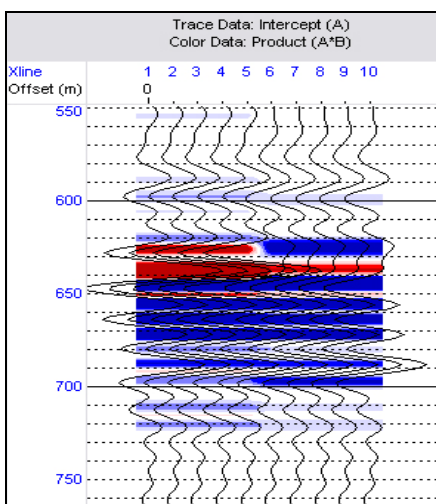


Figure 9. New calculation of the intercept and gradient attributes.

Finally, we examined what can be learned by cross plotting intercept against gradient. The resulting cross plot shows a cluster or "wet trend" about the origin. In addition, we can see anomalous values in the first and third quadrants, with brown, light blue and red colors which should correspond to Class III AVO anomalies and they correspond to 620 up to 640 milliseconds in the presence of gas sands (figure 10).

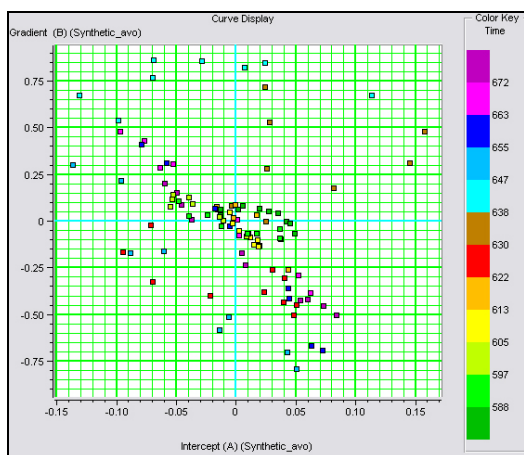


Figure 10. Cross plotting intercept against gradient.

To highlight these regions, the cross plot was divided into two main parts; the wet zone and the gas zone. Figure 11 represents these highlighted zones (one wet zone and three gas zones).

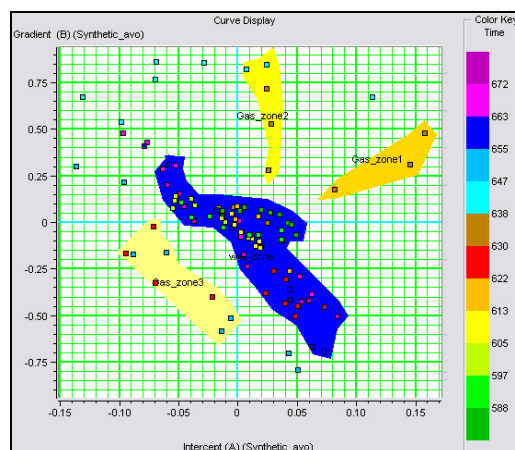


Figure 11. Highlighting wet zone and gas zones.

These main zones have been displayed on the original seismic data (figure 12).

Note that the gas zones are clearly indicated by the yellow regions and wet zones indicated by the blue ones.

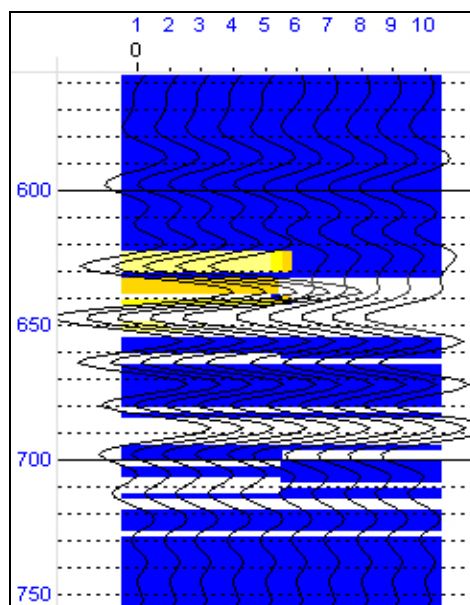
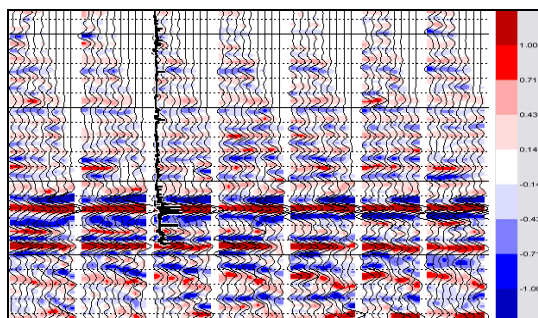


Figure 12. presenting two main zones on the original seismic data.

### 4-3 AVO Analysis on 2D Data

We completed the modeling phase of this project. Part of that analysis was to apply AVO attributes to the synthetic seismograms which were created. In this section, we performed a similar analysis on the real CDP gathers from the 2D data set which ties this well.

At first the amplitude values were displayed as a color scale behind the seismic wiggles (figure 13). The resulting display shows the seismic amplitudes plotted in color behind the wiggle traces.



**Figure 13.** Real CDP gathers from the 2D data set which ties X-well.

Then AVO attribute volumes were produced. In this procedure the first thing we needed to do was specify velocity information to be used in calculating the incidence angles. For this we used a sonic log from the database to read the velocities from it as the velocity control for the AVO attribute calculation.

The result automatically appeared as a color plot (figure 14). The wiggle traces are the intercept traces. The color attribute is the product of intercept and gradient,  $A*B$ . This is most appropriate for a Class III AVO anomaly, and in this case, we can see the strong red (positive) response at the top and base of the gas sand at about 630 milliseconds.

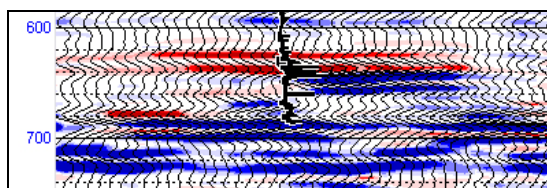


**Figure 14.** AVO attribute calculated for Seismic data.

The final process we applied was to cross plot the calculated Intercept and Gradient. For the range of traces for the cross plot we selected about 60 traces around the anomaly (from CDP 300 up to CDP 360).

The cross plot (figure 15) shows a large wet trend through the origin and the second

and fourth quadrants, as well as anomalies in the first and third quadrants, as expected for a Class III anomaly.

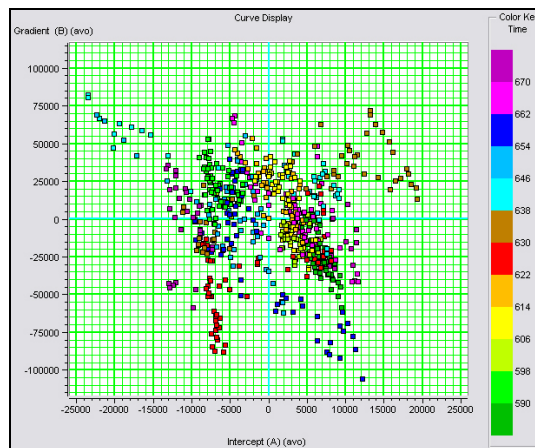


**Figure 15.** Cross plotting intercept against gradient on seismic data.

To highlight these regions, they were divided in two main parts; wet zone and gas zone. Figure 16 illustrates these highlighted zones (one wet zone and two gas zones). The anomalous data in quadrant 3 is the top of the gas sand.

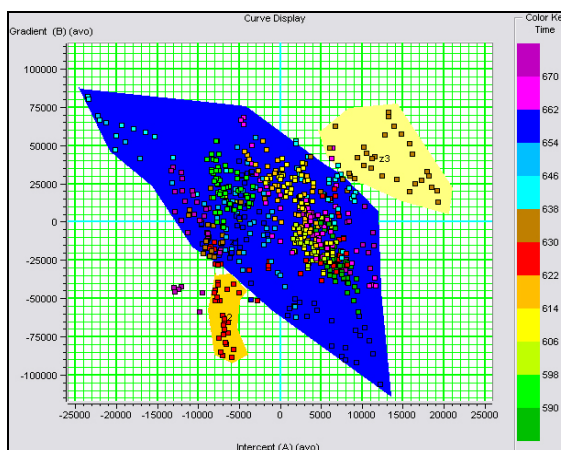


**Figure 16.** Highlighting wet zone and gas zone.

We would like to see where those zones fall on the original seismic data. These two main zones have been displayed on the original seismic data (figure 17). Note that the gas zone is clearly indicated by the yellow regions and wet zone indicated by the blue ones.

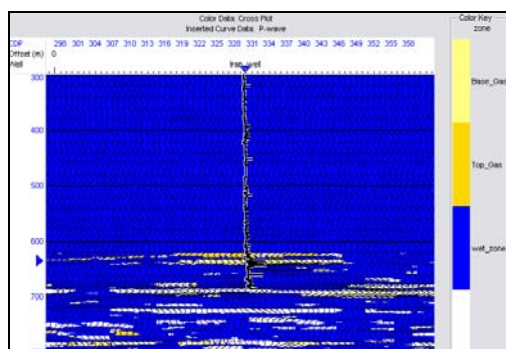


**Figure 17.** Representing of gas and wet zones on the entire data set.

## 5 CONCLUSIONS

An AVO looks for seismic reflection anomalies.

In the first stages of hydrocarbon detection, when there is not enough seismic data, Direct Hydrocarbon Indicators could be useful to reduce the risk of exploration operations. In the regions where they withdraw the primary stages and information from different wells is available the more precise usage of AVO attributes and modeling would be probable. Hence making decisions to drill new wells becomes rather simplified.

AVO analysis could reduce the risk of drilling but for justification, drilling operation is needed.

The reliance on anomaly will be increased by the quality of data, adequate offsets for reflection depth and gathering numerous lines.

Where there is no well as a control point, AVO analysis will not be reliable. Although, AVO analysis is performed on seismic data the potential of AVO analysis as a direct hydrocarbon indicator would be tested and results could be controlled by using well data.

An empirical linear relation between compressional and shear wave velocities was derived from laboratory core analysis data in water saturation condition, which is somewhat similar to Castagna's mudrock line equation. Then S-wave log has been created from P-wave log using the obtained equation, and the resulting Poisson's Ratio log has been displayed.

Comparison between two different synthetic seismograms (wet and gas models), leads to this result that the product of Intercept and Gradient ( $A*B$ ) is the best AVO attribute to distinguish gas from water.

The synthetic seismogram model which was generated from well data shows very good correlation to real seismic data.

An anomaly was detected on AVO attributes of synthetic seismogram at about 630 milliseconds which was confirmed by well log data.

Comparison of different attributes on real seismic data and applying the product of Intercept and Gradient ( $A*B$ ), as an excellent gas indicator lead to finding anomalies at about 630 milliseconds (the time which is expected from synthetic seismogram analysis) and confirmed the presence of the gas.

The study with precise but not so complicated calculations, intends to investigate for probable hydrocarbon plays using 2D seismic data without necessity of structural condition such as anticlines. This kind of study will be a focalization point for future exploration operations.

## ACKNOWLEDGMENT

We would like to thank the Petroleum University of Technology, IFP-School and the professors for facilitating this work.

## REFERENCES

- Bortfeld, R., 1961 Approximation to the reflection and transmission coefficients of plane longitudinal and transverse waves: *Geophys. Prospect.*, 9, 485-502.
- Gassmann, F., 1951, Elastic waves through a packing of spheres: *Geophysics*, **16**, 673-685.
- Castagna, J. P., 1993, Petrophysical Imaging Using AVO: *TLE* **12**, 172-178.
- Castagna, J. P. and Backus, M. M., 1997, Offset-dependent Reflectivity – Theory and Practice of AVO Analysis: Society of Exploration Geophysicists.
- Castagna, J. P., Batzle, M. L. and Eastwood, R. L., 1985, Relationship between compressional wave and shear-wave velocities in clastic silicate rocks:

- Geophysics, **50**, 571-581.
- Castagna, J. P. and Smith, S. W., 1994, Comparison of AVO indicators a modeling study: Geophysics, **59**, 1849-1855.
- Castagna, J. P., Swanz, H. W. and Foster, D. J., 1998, Framework for AVO gradient and intercept interpretation: Geophysics, **63**, 948- 956.
- Foster, D. J., Smith, S. W., Dey-Sarkar, S. and Swan, H. W., 1993, A closer look at hydrocarbon indicators, 63rd ann. mtg. of the SEG, Expanded Abstracts, 731-733.
- Gelfand, V. Ng. P. and Larner, K., 1986, Seismic Lithology Modeling of Amplitude Versus Offset Data: 56th SEG Mtg., Houston, Expanded Abstracts, 332-334.
- Hilterman, F., 1990, Is AVO the Seismic Signature of Lithology?: TLE **9**, 15-22.
- Mamdouh, R. G., 1994, Reservoir Seismology, Pennwell Books.
- Ross, C. P. 2000, Effective AVO crossplot modeling: A tutorial, Geophysics, **65**, 700-711.
- Rutherford, S. R. and Williams, R. H. 1989, Amplitude-versus-offset variations in gas sands: Geophysics, **54**, 680-688.
- Zhijing, W., 2001, Fundamentals of seismic rock physics: Geophysics, **66** (2), 398-412.